A Data-Based Policy Model for Intelligent Turbine Cascade Design

Z. Li, Y. Liu[†], J. G. Yang, H. Q. Wang

School of Energy and Power Engineering, Dalian University of Technology, No. 2 Linggong Road, Ganjingzi District, Dalian 116024,China

†Corresponding Author Email: yanliu@dlut.edu.cn

ABSTRACT

The study of intelligent design methods is becoming a hot topic for the design of turbine cascades. This paper proposes a data-based policy model to achieve intelligent design. To gain a high-quality policy model, empirical equations and "space extending + elitism" are adopted to dynamically optimize database. This guarantees the quality of the model. Compared to traditional optimization design approaches, the proposed method relies on less human experience to design a turbine cascade. Ten different turbine cascades are used to verify this method. Results show that, aerodynamic performance of the cascades redesigned is either the same as or better than that of the traditional cascades. The computing time is reduced by more than one order of magnitude compared to a "CFD + optimization algorithm" or "surrogate model + optimization algorithm" method. With the advantages in computing time and intelligence, the proposed novel method shows the possibility of replacing traditional design methods.

Keywords: Cascade design; Surrogate model; Artificial intelligence; Optimization design; Neural network.

NOMENCLATURE

$AVDR$	Axial Velocity Density Ratio	η	cascade efficiency
g	transformation function of flow angle	θ^*	parameters of policy model
i	incidence angle (unit is degree)	κ	curvature
k_w	control parameter of leading edge wedge angle	λ , μ	control parameters of suction surface
L_{ax}	axial chord length	π	policy model
M	auxiliary points of Bezier Curve	σ_x	axial solidity
Ma	Mach number	Φ	control parameter of iteration
N	number of samples for design variables		
P	control points of Bezier Curve		
Q	number of samples for optimization variables	**Subscript**	
r	leading or trailing edge radius	1	cascade inlet or leading edge
w	1/2 wedge angle	2	cascade outlet or trailing edge
X	design variable group	d	design condition
Y	evaluation variable group	k	blade angle
y	cascade evaluation value	obj	objective
Z	optimization variable group	p	pressure surface
Z_m	modification of Zweifel coefficient	s	isentropic
		v	variable condition
β	flow angle or blade angle		
γ	specific heat ratio	**Acronyms**	
γ_p	stagger angle of pressure surface	CFD	Computational Fluid Dynamics
Δc_β	deviation angle coefficient	DoA	design of artificial intelligence
$\Delta\beta$	turning angle of pressure surface	EIF	Equivalent Inviscid Flow
δ	coefficient related to stagger angle	EXP	experimental
δ_m	deviation rate of massflow	Ori	original
ε	control parameters of pressure surface	RANS	Reynolds-Average Navier-Stokes

1. INTRODUCTION

Turbine cascade design is a complex and iterative process. With the development of computer technology and optimization algorithms, design of turbine cascades and gas turbines is becoming more and more intelligent. Early researchers obtained a series of empirical equations to guide the design. The "intelligence" is described in the form of equations (Pritchard 1985) to simplify the work of designers. In the 1990s, the combination of computational fluid dynamics and an optimization algorithm ("CFD + optimization algorithm") was applied to design turbine cascades. This method gradually became a widely used design method and it also has been continuously developed (Shelton *et al.* 1993; Sonoda *et al.* 2006; Giel 2008; Chatel *et al.* 2019). Although this approach does not make use of much human expert experience, the computational cost is expensive. To solve the problem, an improved method i.e. "surrogate model + optimization algorithm" (Pierret and Van den Braembussche. 1999) was proposed. A surrogate model is used to replace CFD analysis. Hence the computing time is reduced by several orders of magnitude (Kosowski *et al.* 2010). For turbine cascade design, different surrogate models such as artificial neural networks (ANN) (Pierret and Van den Braembussche. 1999; Kosowski *et al.* 2010) and support vector machines (SVM) (Anguita *et al.* 2003) were studied. No surrogate model is absolutely superior though ANN is the most widely used one.

Undoubtedly, surrogate models can reduce computing time. However, model construction is time consuming. Most surrogate models can only be used once because they are constructed for a specific cascade. Taking model construction time into account, "surrogate model + optimization algorithm" is still an expensive method. Little work has been done on how to reduce the time of model construction in turbomachinery. Nevertheless, some researchers have tried to improve model adaptation to more cascades. A common method is to construct a richer CFD database (Kosowski *et al.* 2009). Another method is to construct a cascade generation policy (Clark 2019) independent of optimization algorithms. This kind of method is called a policy model in this paper. A policy model learns knowledge from data and uses the knowledge to design a product.

Policy model construction includes database construction and data learning. For the turbine cascade design, almost all the time consumed comes from database construction. With regards to database construction, there are two difficulties. The first is how to determine the value ranges of variables describing a turbine cascade. It has been a persistent problem for researchers since the era of "CFD + optimization algorithm" (Moroz *et al.* 2004). Ranges from upper bound to lower bound for variables decide the feasibility and universality of a method. To select reasonable value ranges, priori knowledge and human expert experience are needed. The second difficulty is how to get high quality data. The existing optimization design methods cannot

afford the computing time of generating the database. Therefore, a more efficient selection strategy is needed to select "good" data into the database.

Based on the above discussion, the most important problem for the policy model method is database construction. An intelligent turbine cascade design method with empirical equations and "space extending + elitism" is proposed to solve the problem. The equations translate human experience into a form that artificial intelligence (AI) can understand. "Space extending + elitism" uses optimization and selection to store the best human experience into AI. For a design task, using the AI experience directly is more efficient than "CFD + optimization algorithm". The proposed method aims to shorten computing time to several minutes to design a cascade. It also provides a feasible intelligent design idea for other fields.

2. DESIGN PROCESS

2.1 Mathematical Expression

The design variable group X (design requirements), optimization variable group Z (design schemes), and evaluation variable group Y (aerodynamic performance) are essential elements of a design. The process of the intelligent turbine cascade design can be divided into two steps. The first is the mathematical definition of a cascade design shown in Eq. (1). The second is to construct a database and obtain the best policy model. The policy model is a function of design variable group X and the optimal schemes Z^*. The mathematical expression of the function is shown in Eq. (2).

$$Y = f(X, Z) \tag{1}$$

$$Z^* = \pi_{\theta^*}(X) \tag{2}$$

To realize the two processes above, the following problems must be solved:

Determine the ranges of variables in X;

Determine the initial ranges of variables in Z;

Specify the mathematical expression of the design and evaluation function f;

Choose an intelligent policy model π;

Construct a cascade database and obtain the optimal policy parameter θ^* by data learning.

2.2 Design Variable Group X

Based on typical turbine design references (Aungier 2006a; Kacker and Okapuu 1982; Aungier 2006b). X consists of 7 sets of variables given in Eq. (3)

$$X = \{\beta_{1d}, \beta_{2obj}, Ma_2, AVDR, \gamma, \sigma_x, r_2/L_{ax}\} \tag{3}$$

Where β_{1d} is inlet flow angle (based on axial direction), β_{2obj} is objective outlet flow angle, Ma_2 is outlet Mach number, $AVDR$ is axial velocity density ratio, γ is specific heat ratio, σ_x is axial solidity, and r_2/L_{ax} is the ratio of trailing edge radius to axial chord length.

The reason why β_{1d}, β_{2obj}, Ma_2, $AVDR$ and γ are associated to X is because they determine the operating conditions of a cascade. Geometric

variables involving σ_x and r_2/L_{ax} are also involved in the design variable group X, since they determine the structural constraints of a cascade. The effect of Reynolds number will not be considered, because the effect of Reynolds number is negligible for most traditional turbines. The inlet Reynolds number (based on unit length) of 8×10^6 is selected in this paper. Furthermore, the influence of the axial chord length L_{ax} is not considered due to the neglected influence of Reynolds number. The cascades with different axial chord lengths can be obtained by a scaling transformation.

Velocity is a direct reflection of flow conditions, and the ratio of the velocity components can be expressed by simple trigonometric functions. So, all the angles are transformed to cosine functions. The transformation functions g_1 and g_2 of inlet and outlet flow angles are given in Eq. (4),(5).

$$\beta_{1d} = \begin{cases} \arccos\left(2 - g_1\left(\beta_{1d}\right)\right) & , g_1\left(\beta_{1d}\right) > 1 \\ -\arccos\left(g_1\left(\beta_{1d}\right)\right) & , g_1\left(\beta_{1d}\right) \leq 1 \end{cases} \quad (4)$$

$$\beta_{2obj} = \arccos\left(g_2\left(\beta_{2obj}\right)\right) \quad (5)$$

In addition, a constraint "$|\beta_{1d}| < \beta_{2obj}$" is used to exclude most unreasonable design conditions. Eq. (6) is applied to construct the transformation function between the axial solidity σ_x and the modification of Zweifel coefficient Z_m. The use of Z_m can exclude most unreasonable design conditions, benefiting the database construction.

$$\sigma_x = \begin{cases} \dfrac{2\cos^2\beta_{2obj}\left|\tan\beta_{2obj} - \tan\beta_{1d}\right|}{Z_m \cos\left(\dfrac{\beta_{1d} + \beta_{2obj}}{2}\right)}, \beta_{1d} < 30 \\ \\ 0.75\left(0.6 - Z_m\right) + 1.0 \qquad , otherwise. \end{cases} \quad (6)$$

Table 1 shows the specific ranges of the variables in X, where all the angles are defined based on axial direction.

Table 1 Design variable ranges and constraints of turbine cascades

Variables	Ranges
$\beta_{1d}[deg] \& g_1(\beta_{1d})$	[-69.5,69.5]&[0.35,1.65]
$\beta_{2obj}[deg] \& g_2(\beta_{2obj})$	[40,80]&[0.174,0.766]
Ma_2	[0.3,1.3]
$AVDR$	[0.7,1.25]
γ	[1.2,1.67]
Z_m	[0.6,1.4]
r_2/L_{ax}	[0.005,0.03]
Constraint	$|\beta_{1d}| < \beta_{2obj}$

The ranges of β, Ma_2 and $AVDR$ are determined based on (Aungier 2006a,b; Kacker and Okapuu 1982). The fluid types with the range of γ include air, gas, water steam, helium and so on. The range of Z_m is larger than the recommended range of the traditional design method. The upper value of r_2/L_{ax} is bigger than that of traditional turbines. Usually, only some micro turbines use the value of 0.03.

Some unconventional turbine cascades, such as hypersonic turbine cascades (Colclough 1966a,b) and ultra-high load turbine cascades (Tsujita and Kaneko 2019) are not involved in this paper.

2.3 Cascade Profile Parameterization

Parameterization is an essential process which directly determines the number of optimization variables (Li and Zheng 2017). These variables compose the optimization variable group Z. A parameterization method is proposed, and the initial ranges of the variables in Z will be specifically discussed later.

As shown in Fig. 1, the cascade profile is connected by two arcs and two Bezier curves, in which the suction surface is a 5th-order Bezier curve, and the pressure surface is a 4th-order Bezier curve. The parameterization causes the profile having four connecting points, so continuity conditions of the points must be considered. The continuity conditions given in this paper are as follows: the G^2 continuity condition needs to be satisfied at the connecting points of the pressure surface and leading edge, and the G^1 continuity condition needs to be satisfied at the other three connecting points.
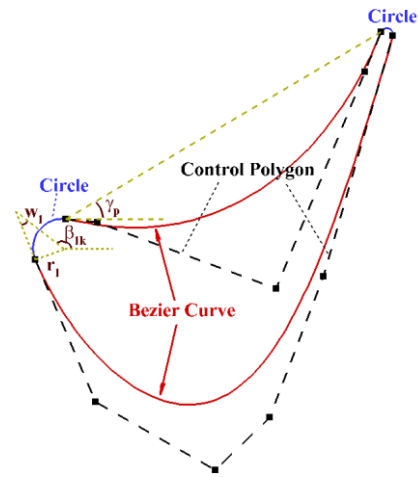

Fig. 1. Schematic of turbine cascade profile parameterization.

Although the parameterization method mentioned above is not complex, it is not easy to determine the variable ranges. To simplify the expression of the formulas, only the condition $\beta_{2k} > 0$ is discussed, where the β_{2k} is outlet blade angle. Under the condition of $\beta_{2k} < 0$, the cascade profile can be simply reversed to achieve the objective.

2.4 Leading and Trailing Edges

For an arc in a two-dimensional plane, its position and shape can be completely determined by five parameters $\{\beta, w, r, x, y\}$. The cascade position determines the leading edge arc (x_1, y_1), and the leading edge radius r_1 is determined by Eq. (7).

$$r_1 = 0.84 L_{ax} \cos\beta_{1d} / \sigma_x \quad (7)$$

The blade angle β_{1k}, 1/2 wedge angle w_1, and inlet flow angle β_{1d} satisfy the equation given in Eq. (8).

$$tan \, \beta_{1d} = \frac{tan(\beta_{1k} + w_1) + tan(\beta_{1k} - w_1)}{2} \qquad (8)$$

There are two unknown variables β_{1k} and w_1 in Eq. (8). A variable k_w and two procedure parameters β_{p1} and β_{p2} are used. The definitions of these parameters are given in Eq. (9).

$$\beta_{p1} = \beta_{1k} + w_1$$

$$\beta_{p2} = \beta_{2k} - w_2$$

$$k_w = \frac{\beta_{p1} - \beta_{1d}}{\beta_{p2} - \beta_{1d}} \qquad (9)$$

The outlet 1/2 wedge angle w_2 is a known constant, which will be discussed later. So far, the parameterization of leading edge can be expressed by a variable k_w. According to the characteristic of the pressure surface and definition of k_w, the value range of k_w being 0 to 1 is reasonable. It is easier to obtain a more reasonable cascade profile by narrowing the range as $k_w \in [0.2, 0.6]$.

The coordinate of the trailing edge (x_2, y_2) can be obtained from (x_1, y_1), L_{ax}, and γ_p, where L_{ax} can take any value as the reference length. γ_p is the stagger angle of the pressure surface and can be obtained by an iterative calculation of leading edge, trailing edge, and pressure surface. The iterative calculation process will be discussed later. The trailing edge 1/2 wedge angle w_2 has a significant influence on trailing edge thickness and trailing edge loss. The increase of w_2 always leads to the increase of aerodynamic loss, so it is more reasonable to give w_2 a constant value instead of a range. The value between 0 and 7° is common. Considering the thickness and aerodynamic loss, the value is given in Eq. (10).

$$w_2 = 3° \qquad (10)$$

The trailing edge radius r_2 is a geometric constraint, which is included in the design variable group X. The blade angle β_{2k} is calculated from the objective outlet flow angle β_{2obj} and the deviation angle Δc_β. The mathematical expression for β_{2k} is given in Eq. (11).

$$\cos \beta_{2k} = \cos \beta_{2obj} + \Delta c_\beta \qquad (11)$$

where β_{2obj} can be obtained from the design variable group X. The deviation angle Δc_β represents the deviation between the blade angle and the flow angle to a certain extent. The variable range of Δc_β is easy to determine. This paper takes the range of $\Delta c_\beta \in [-0.2, 0.2]$. So the parameterization of the trailing edge is expressed by one variable Δc_β.

2.5 Pressure Surface

The pressure surface consists of a 4th-order Bezier curve. As shown in Fig. 2, suppose that the connection point of the pressure surface and the leading edge is P_0, and the connection point of the pressure surface and the trailing edge is P_4. The auxiliary point M can be obtained by the G^1 continuity condition.
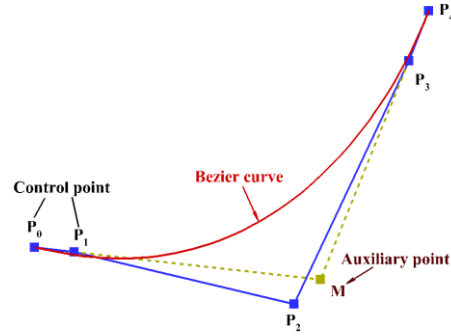
Fig. 2. Schematic of pressure surface Bezier Curve.

A vector $\vec{\varepsilon}$ is defined to construct the function of pressure surface, as shown in Eq. (12).

$$P_2 = \frac{(\varepsilon_1 + \varepsilon_2)M + (1 - \varepsilon_1)P_0 + (1 - \varepsilon_2)P_4}{2}$$

$$P_3 = \varepsilon_3 M + (1 - \varepsilon_3)P_4$$

$$\vec{\varepsilon} = (\varepsilon_1, \varepsilon_2, \varepsilon_3) \qquad (12)$$

$$\varepsilon_1, \varepsilon_3 \in (0,1)$$

$$\varepsilon_2 \in (1, +\infty)$$

Eq. (13) is obtained by G^2 continuity condition at the leading edge and pressure surface connection point.

$$P_1 = P_0 + \frac{4r_1 \left| \overrightarrow{P_0M} \times \overrightarrow{P_0P_2} \right|}{3 \left| \overrightarrow{P_0M} \right|^{1.5}} (M - P_0) \qquad (13)$$

where r_1 is leading edge radius. So far, all the control points of the pressure surface are expressed by $\vec{\varepsilon}$. The pressure surface has a specific turning angle, and the flow near the pressure surface is always subsonic for traditional turbine cascades. Under flow conditions, the aerodynamic loss near the pressure surface comes from a large local flow turning caused by a large change of local curvature. Therefore, a function between the curvature distribution and $\vec{\varepsilon}$ needs to be established. To establish the function, two parameters are defined as shown in Eq. (14).

$$\Delta\beta = \beta_{p2} - \beta_{p1}$$

$$\delta = \frac{2(\gamma_p - \beta_{p1})}{\Delta\beta} - 1 \qquad (14)$$

where β_{p1} and β_{p2} are defined in Eq. (9), γ_p is shown in Fig.1. Thus, the curvature of any point on the pressure surface is a function defined in Eq. (15).

$$\kappa = \kappa(\Delta\beta, \delta, \kappa_0, \vec{\varepsilon}, t) \qquad (15)$$

where t is the parameter of Bezier curve. $\kappa_0 = -1/r_1$ is the curvature at point P_0. The equation takes the sign of the curvature into account and takes $\kappa_0 < 0$. A min-max optimization function is proposed as shown in Eq. (16) avoiding sharp local changes of the blade profile.

$$\vec{\varepsilon}_{opt} = \arg\min_{\vec{\varepsilon}} \max_t \left(\kappa \,|\, \Delta\beta, \delta, \kappa_0 \right) \tag{16}$$

It is found that the influence of κ_0 on $\vec{\varepsilon}_{opt}$ is negligible. Finally, an interpolation table is constructed to solve $\vec{\varepsilon}_{opt}$ by inputting δ and $\Delta\beta$. Therefore, the parameterization of the pressure surface is expressed by adding a new variable δ. In this paper, the range of δ is given as $\delta \in [-0.5, 0.5]$.

2.6 Suction Surface

The suction surface consists of an n-order Bezier curve. However, it is found that when $n>5$, the increase of curve order will no longer get obvious aerodynamic performance benefit, so $n=5$ is chosen. In this paper, the suction surface only uses convex Bezier curves, which can suit most of the design requirements, and that is why the method cannot be applied to hypersonic cascades. Fig. 3 depicts the geometric schematic of the suction surface Bezier curve.
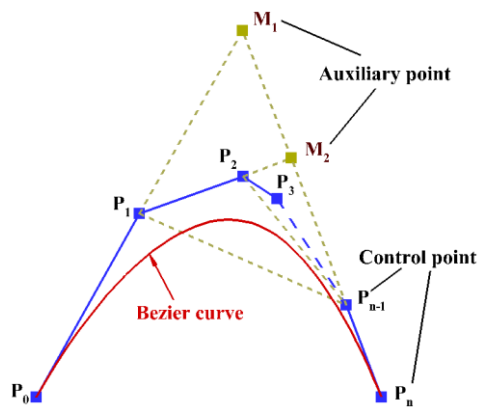
Fig. 3. Schematic of suction surface Bezier Curve.

The connection point of the suction surface and the leading edge is P_0, and the point of the suction surface and the trailing edge is P_n. The auxiliary point M_1 is obtained by G^1 continuity condition. Other auxiliary points and control points are obtained by Eq. (17).

$$P_1 = \lambda_1 \left(M_1 - P_0 \right) + P_0$$

$$P_{n-1} = \mu_1 \left(M_1 - P_n \right) + P_n$$

$$P_i = \lambda_i \left(M_{i-1} - P_{i-1} \right) +$$

$$\mu_i \left(1 - \lambda_i \right) \left(P_{n-1} - P_{i-1} \right) + P_{i-1} \tag{17}$$

$$M_i = line \left(P_n P_{n-1}, P_i P_{i-1} \right)$$

$$i \in \{2, 3, \ldots, n-2\}$$

$$\lambda_i, \mu_i \in [0,1]$$

where P is the control point group of Bezier curve, M is a defined auxiliary point group, *line* is a function to find the intersection of two lines. $\vec{\lambda}$ and $\vec{\mu}$ are two defined vectors of suction surface. According to the assumption of the convex curve, $\lambda_i \in [0,1]$ and $\mu_i \in [0,1]$ are taken. Thus, the parameterization of the suction surface is expressed by two vectors $\vec{\lambda}$ and $\vec{\mu}$.

2.7 Optimization Variable Group Z

By analyzing the process of parameterization, it can be seen that for a specific design requirement, nine independent variables need to be given to determine a complete cascade profile. Table 2 shows the initial ranges of optimization variables, which have already been discussed in detail. The ranges will be adjusted by the policy model to eliminate bad cascades.

Table 2   Initial ranges of optimization variables

Variables	Ranges
Δc_β	[-0.2,0.2]
k_w	[0.2,0.6]
δ	[-0.5,0.5]
$\lambda_1, \lambda_2, \lambda_3$	[0.0,1.0]
μ_1, μ_2, μ_3	[0.0,1.0]

2.8 Evaluation Variable Group Y

Three demands are considered to evaluate the aerodynamic performance of turbine cascades: the requirements of massflow, power, and structural constraints need to be satisfied; The aerodynamic performance is good enough; The performance under off-design conditions is not bad. How to comprehensively evaluate the three demands is a problem in multi-point turbine cascade design. Some algorithms have the advantages of solving multi-objective problems, such as the second-generation (Deb *et al.* 2002) and the third-generation (Deb and Jain 2013; Jain and Deb 2013) multi-objective genetic algorithms. However, they will lead to unacceptable computing time for the big data needed in this paper. Therefore, a aerodynamic performance evaluation equation based on multi-point design experience is given, as shown in Eq. (18).

$$y = 0.5\eta_d + 0.5\eta_v - 0.1\delta m$$

$$\delta m = \left| \frac{\cos\beta_2 - \cos\beta_{2obj}}{\cos\beta_{2obj}} \right| \tag{18}$$

$$\eta = \left(\frac{Ma_2}{Ma_{2s}} \right)^2$$

In the above, δ_m is deviation rate of mass flow, η is efficiency of the cascade, defined as the square of the ratio of outlet Mach number to outlet isentropic Mach number, and β_2 is outlet flow angle. The subscript d represents the design condition, and v represents the condition with positive attack and different outlet Mach number of off-design conditions. Moreover, y represents the evaluation value of aerodynamic performance. The evaluation variable group Y is composed of the evaluation value y.

The inlet flow angle β_{1v}, and outlet Mach number Ma_{2v} under the condition v are given by design experience as shown in Eq. (19). Except β_{1v} and

Ma_{2v}, the others are equal to the variables under design conditions.

$$\beta_{1v} = \arctan\left(\tan\beta_{1d} - 0.5\right)$$

$$Ma_{2v} = \begin{cases} Ma_{2d} + 0.2 & Ma_{2d} < 0.8 \\ 1.0 & 0.8 \le Ma_{2d} < 1.2 \\ Ma_{2d} - 0.2 & Ma_{2d} \ge 1.2 \end{cases} \quad (19)$$

The aerodynamic parameters involved above can be obtained by a quasi-three-dimensional numerical simulation method using Multiple Blade Interacting Streamtube Euler Solver (MISES) (Youngren 1991; Drela and Giles 1987). The solver uses an Equivalent Inviscid Flow (EIF) model to simulate the flow field, where both the boundary layers and shock waves can be captured. The advantage of using EIF is fast calculation, though it is less accurate than more widely used methods such as RANS.

3. POLICY MODEL

The policy model is used to solve a high dimensional regression problem shown in Eq. (2). The artificial neural networks (ANN), being a widely used regression model, is adopted to implement the policy. The ANN uses Error Back Propagation(BP) to update the parameters of the network until a minimum regression error.

A database updating method is proposed to gain high quality data. The method is achieved by a learning framework called "space extending + elitism". As shown in Fig. 4, the framework consists of four parts: policy network, space extending process, design simulation, and selection of elites. The inputs include the number of iterations, the number of data N and Q, the variable ranges of X, the initial variable ranges of Z, and the updating rule of the control parameter of iteration Φ which controls the convergence rate and model precision. The variable ranges of X and Z have already been discussed. The values of N, Q and Φ are summarized in Table 3.

Table 3 Values of the iterative parameters during the model construction

Iteration	N	Q	Φ
1	2000	50	----
2	4000	50	0.35
3	4000	100	0.25
4	4000	100	0.15
5	4000	80	0.1

For an iterative step, the variables in X are sampled using Latin hypercube sampling method, and the number of samples is N. The sampling process is repeated enough times to get the distribution of the samples with the max-min Mahalanobis distance, which is an important evaluation of the sample quality. The process effectively ensures the spatial uniformity of the samples, though the computing time increases a few minutes, which is negligible compared to the whole database construction time.
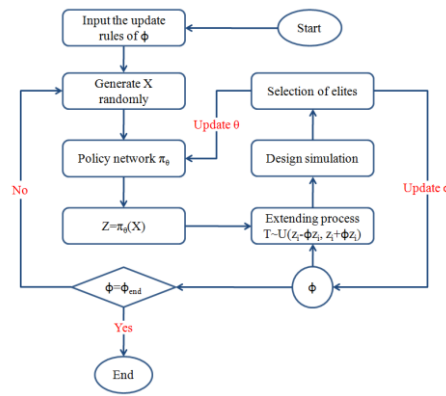
Fig. 4. Framework of database construction.

After the design variable group X is input in the policy model, N samples in the optimization variable group Z are obtained according to Eq. (2). The policy model is a fully connected ANN with four layers (including input and output layers). The number of neurons in each layer is chosen as 7, 40, 50, and 9, respectively. It was found that more neurons did not increase the prediction precision in this study. The output layer activation function is *Sigmoid* shown in Eq. (20). The activation function of hidden layers is *Selu* (Klambauer *et al*. 2017). It can adaptively realize the data standardization of the hidden layers. The mathematical expression of *Selu* is shown in Eq. (21).

$$Sigmoid\left(x\right) = \frac{1}{1 + e^{-x}} \quad (20)$$

$$Selu\left(x\right) = \lambda \begin{cases} x & if \ x > 0 \\ \alpha e^x - \alpha & otherwise \end{cases} \quad (21)$$

$$\lambda = 1.0507 , \quad \alpha = 1.7326$$

N numbers of quasi-elite samples are gained. To gain better elites, a search process centered on quasi-elites Z_i is carried out. The search space follows a uniform distribution shown in Eq. (22). Each T_i is filled with Q numbers of samples, so the total number of the samples is $N \times Q$.

$$T_i\left(X = X_i\right) \sim U\left(Z_i - \phi Z_i, Z_i + \phi Z_i\right) \quad (22)$$

The extended data is input to the design simulation process. Subsequently the evaluation value of each sample can be obtained. During selection of elites, the sample with the highest evaluation value in each T_i is maintained. Thus, N quasi-elites are replaced by better elites, so that the quality of the database is improved. Finally, the new elites are used to update the parameters of the policy model. Then, an iterative step has been completed.

The iteration process above will be carried out for a while. With the increase in iteration cycles, the control parameter Φ decreases so that the variable ranges in Z will be narrowed, and finally the optimal parameters of the policy model are found and locked.

In general the policy model can generate good design schemes. To solve the over-fitting or

under-fitting problem of any surrogate model and to improve the quality of the intelligent turbine cascade design further, an optimization process is applied based on the scheme designed by the policy model. The contribution of the optimization is to eliminate the fitting error of the surrogate model. Δc_β, k_w and δ represent outlet blade angle, leading edge wedge angle and stagger angle of cascades respectively. These three variables are optimized by dozens of EIF simulations with the objective function shown in Eq. (18). Usually, the computing time of ANN is negligible and a single EIF simulation takes 3 to 15 seconds for different cases. So, the total time for a turbine cascade design is only several minutes with a single CPU core.

Table 3 shows the values of N, Q and Φ in this study. About 1.4 million design simulations were carried out. To decrease computational cost, 52 CPU cores (2.1GHz) were used for the model framework with good parallel computing characteristics. The time consumption of the model construction was about 4 days which is longer than that of traditional models. However, compared to the tradition models which were constructed for a specific cascade, the proposed policy model in the current study can be used for almost all the traditional turbine cascades included in Table. 1. The increase in the time consumption of the model construction is worth it in terms of universality improvement of the policy model.

For cascade design, dozens of design simulations are required for the method in this paper, hundreds of design simulations for "CFD surrogate model + optimization algorithm" (Lee *et al.* 2014; Waesker *et al.* 2020) methods and more times for modeless methods. So, the proposed method reduces the computing time by at least one order of magnitude compared to the widely used methods.

4. APPLICATION OF THE PROPOSED POLICY MODEL

To verify this novel method, ten turbine cascades are designed and compared with some typical cascades to show that the policy model is intelligent and the cascades designed have good aerodynamic performance. These typical cascades are called "Ori" (Original). Ori_Case1 from a turbine institute has not been published. Ori_Case2 is from (Bryce *et al.* 1985). Ori_Case3 and Ori_Case4 are from (Behr 2007). The other cases are successively from (Sonoda *et al.* 2006; Kiock *et al.* 1986; Meng *et al.* 2019; Hodson and Dominy 1987; Thulin *et al.* 1982; Chatel *et al.* 2019). These cascades can be divided into two classes roughly. Ori_Case1, Ori_Case5 and Ori_Case10 were obtained from the "CFD + optimization algorithm" method. The others were designed based on human experience. The differences between the cascades can be found in the detailed design requirements and geometric profiles given in Appendix.

The redesigned ten cascades using the policy model are named as DoA_Case1 to DoA_Case10. To compare the aerodynamic performance of the Ori

and DoA cascades, Reynolds Averaged Navier Stokes equations (RANS) were conducted. The NUMECA-FINE-Turbo software was used to simulate flow fields. Experimental (EXP) data for Ori_Case1 was used to verify the predictive accuracy of RANS. The blade height of the test cascade, Ori_Case1, is 160mm. Four five-hole probes are distributed within a pitch. The measuring position is 28mm behind the trailing edge, at mid span of the blade height. For supersonic flow, the measurement results are corrected based on the assumption that a normal shock wave forms at the probe. For the CFD, a single-channel is used as the computational domain. A 3D straight blade model is adopted. The number of grid nodes is about a million. The SST turbulence model with wall functions is used, and the equivalent roughness height is set as 1 micrometer. The aspect ratio is 3.5. Fig. 5 compares predicted total pressure loss coefficients and measured ones. The results show that the CFD prediction is reliable.
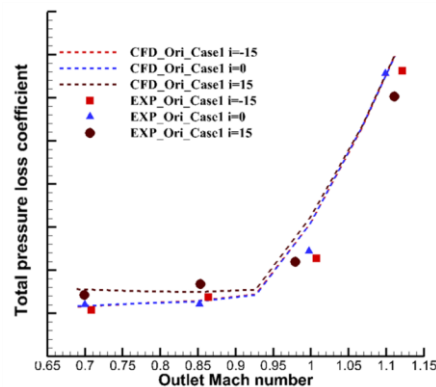

Fig. 5. Comparison of experimental data and CFD results for Ori_Case1.

For any case, the outlet flow angle β_2 should be equal to the objective value β_{2obj}. However, it is acceptable that the outlet flow angle deviations of the ten designed cascades are all less than 1 degree, the largest δ_m is 3.6% and the average δ_m is 1.6%. For more comparisons, the profiles and total pressure loss coefficients are shown in Fig. A in Appendix. Mach distributions of the cascades are shown in Fig. B in Appendix. These results include the operating conditions with different incidence angle (i) and outlet Mach number. For Case1 and Case5, the aerodynamic performance is not much different between the Ori and DoA cascades. For Case10, the DoA cascade performs better than the Ori under relatively high Mach number and worse under lower Mach number. The three Ori cascades are designed by researchers with "CFD + optimization algorithm" method. It means that the proposed policy model method can achieve the level of optimization design. For the other cases, the DoA cascades perform about the same or better. For Case2, Case3, Case4 and Case7, the DoA cascades perform better. The reason is that the DoA cascades obtain more reasonable Mach number distributions than those of Ori. To some extent, these cases prove that the policy model proposed in this paper has advantages on optimization.

5. CONCLUSIONS

The processes or steps of how to construct an intelligent surrogate model, i.e. policy model has been introduced. Ten cascades have been redesigned to verify this policy model. Predicted aerodynamic performances for the redesigned and original cascades have been compared. Some conclusions can be drawn as follows:

"Space extending + elitism" and empirical equations can construct high quality database. "Space extending + elitism" can obtain the expert coefficients of the equations more efficiently than traditional methods. The coefficients can be stored in an ANN policy model. Once the policy model has been constructed, it is intelligent enough to complete a design task for a designer without any prior knowledge

Compared to the "surrogate model + optimization algorithm" method, the current obtained policy model can replace the optimization algorithm. Computing time is reduced by more than one order of magnitude. Less human expert experience is required and cascades with good aerodynamic performance can be gained. These advantages demonstrate a potential for the new method to replace traditional design methods.

APPENDIX

Table. A Design requirements of ten turbine cascades
(Note: the unit of angle is degree, the unit of length is meter and the β_2 is outlet flow angle from RANS)

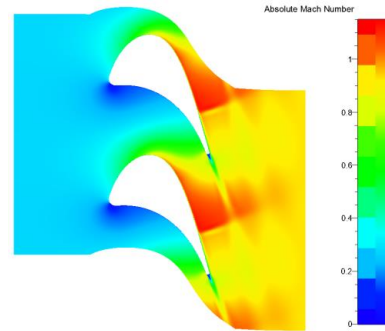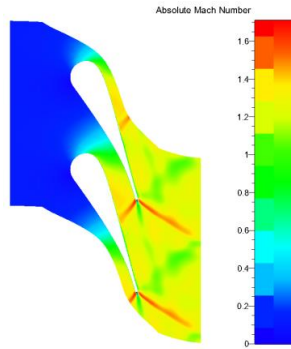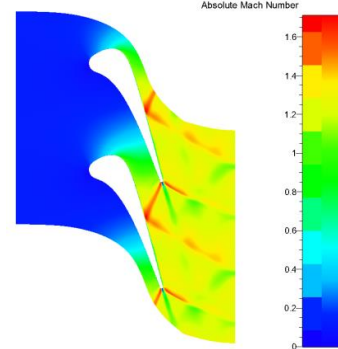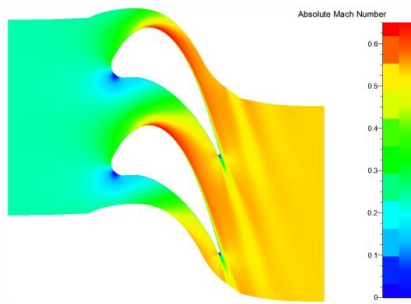|	Case1	Case2	Case3	Case4	Case5	Case6	Case7	Case8	Case9	Case10
γ	1.4	1.4	1.4	1.4	1.4	1.4	1.4	1.4	1.4	1.4
β_1	48.5	0	52.4	0	65	30	25	-38.8	0	0
β_{2obj}	-72.3	-75.2	-71.8	75.3	-69.1	-67.1	-60.3	55.1	79.7	-75.6
β_2	-72.1	-74.7	-71.9	75.5	-68.7	-68.0	-60.3	55.7	79.6	-75.9
Ma_2	0.87	1.25	0.53	0.55	1.15	0.9	0.7	0.71	0.92	0.85
$AVDR$	1.0	1.0	1.0	1.0	1.0	1.0	0.7	1.0	1.0	1.0
$Pitch$	0.061	0.045	0.042	0.063	0.042	0.042	0.055	0.031	0.1	0.062
L_{ax}	0.0499	0.0314	0.0463	0.0492	0.0562	0.048	0.0649	0.0518	0.0429	0.0363
r_2/L_{ax}	0.0166	0.0194	0.0121	0.0145	0.0187	0.0303	0.014	0.0065	0.0198	0.0207
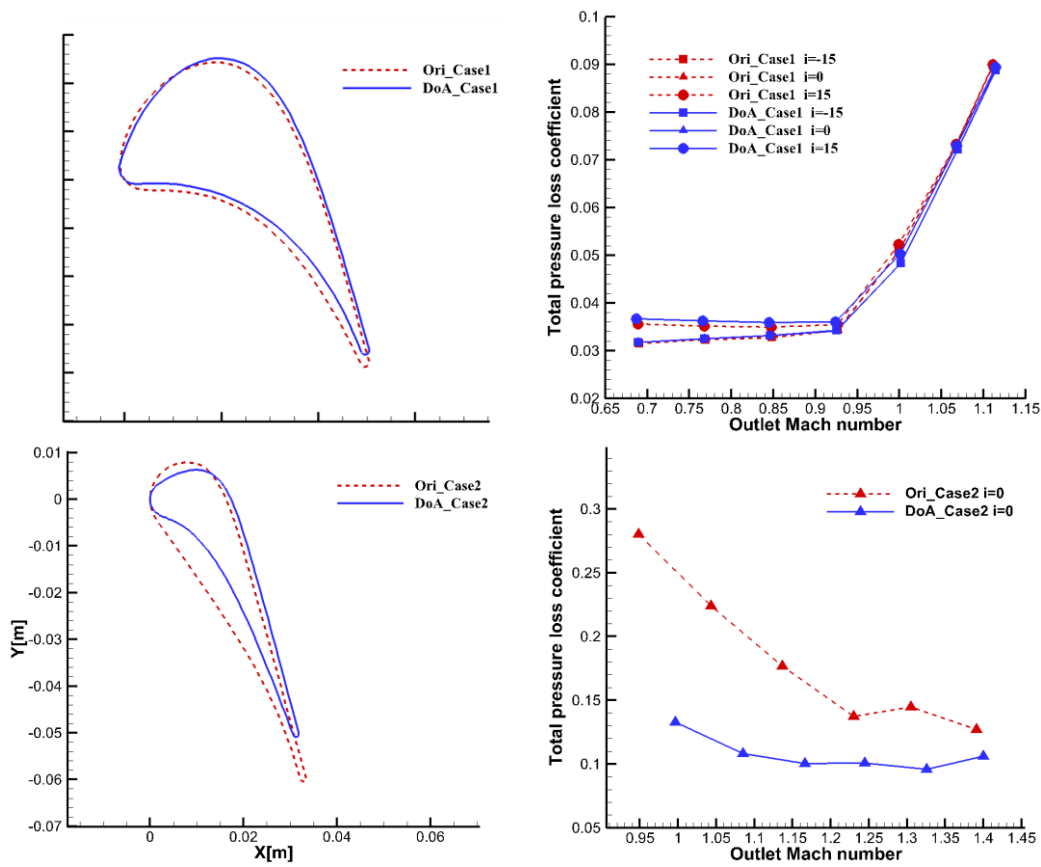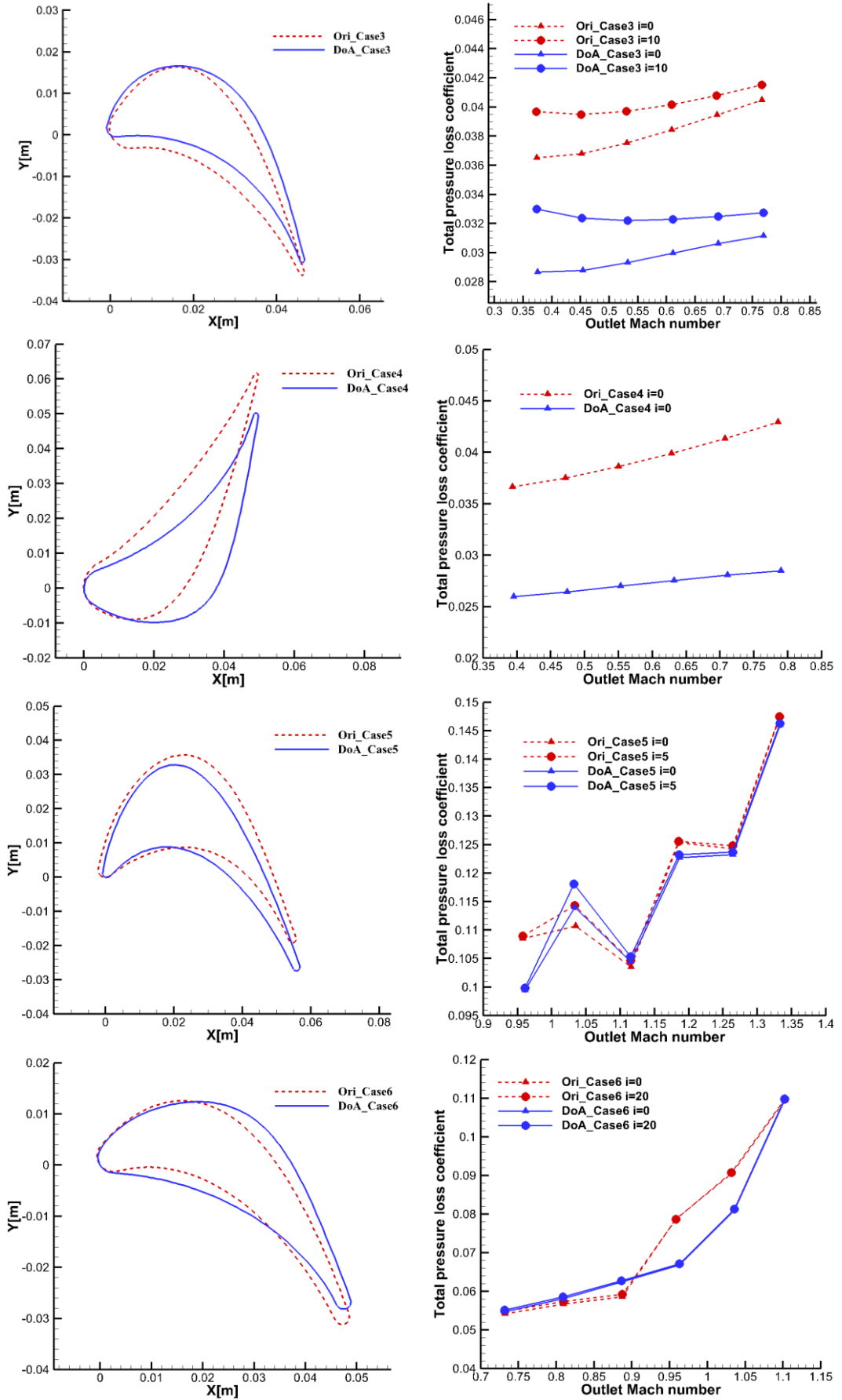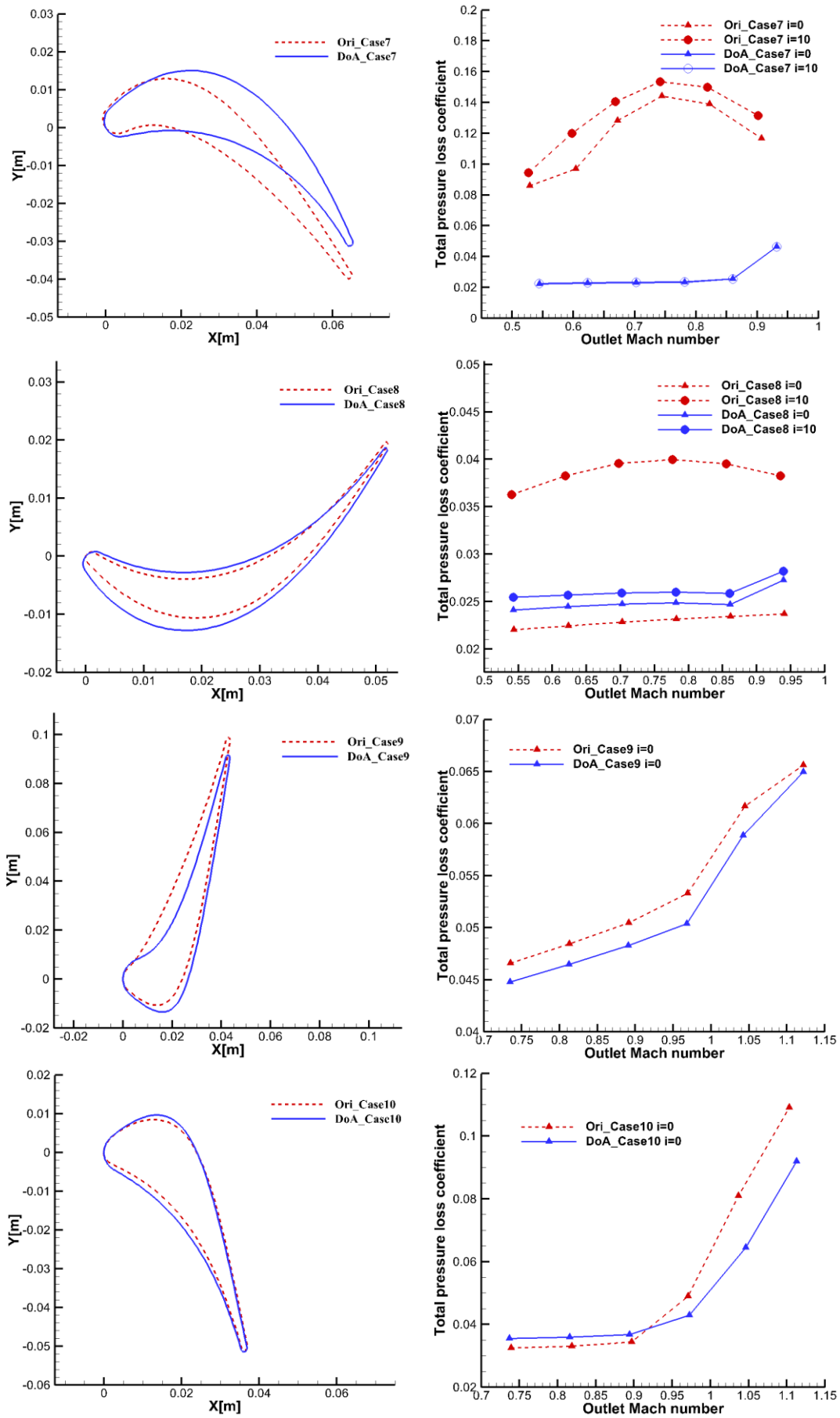
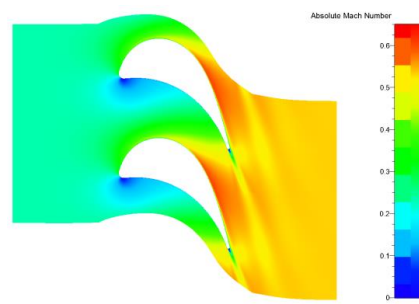**Fig. A. Comparisons of cascade profiles and total pressure loss coefficient.**
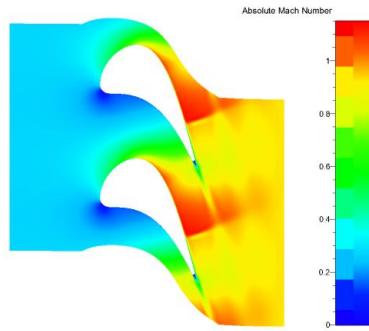
Ori_Case1

DoA_Case1

Ori_Case2

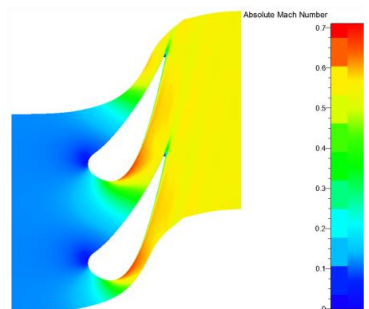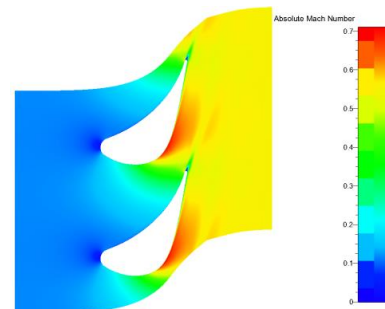DoA_Case2

Ori_Case3

DoA_Case3

Ori_Case4

DoA_Case4

Ori_Case5
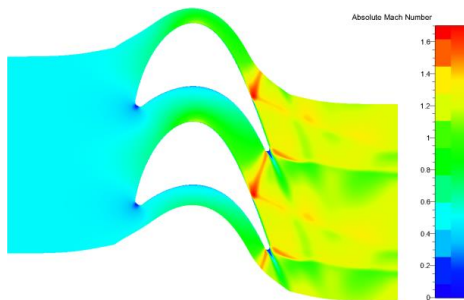
DoA_Case5

Ori_Case6
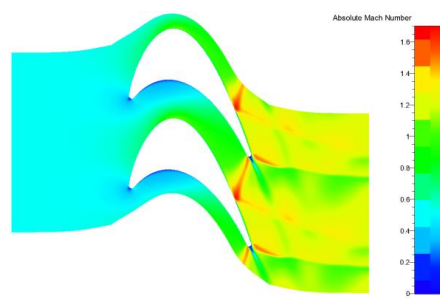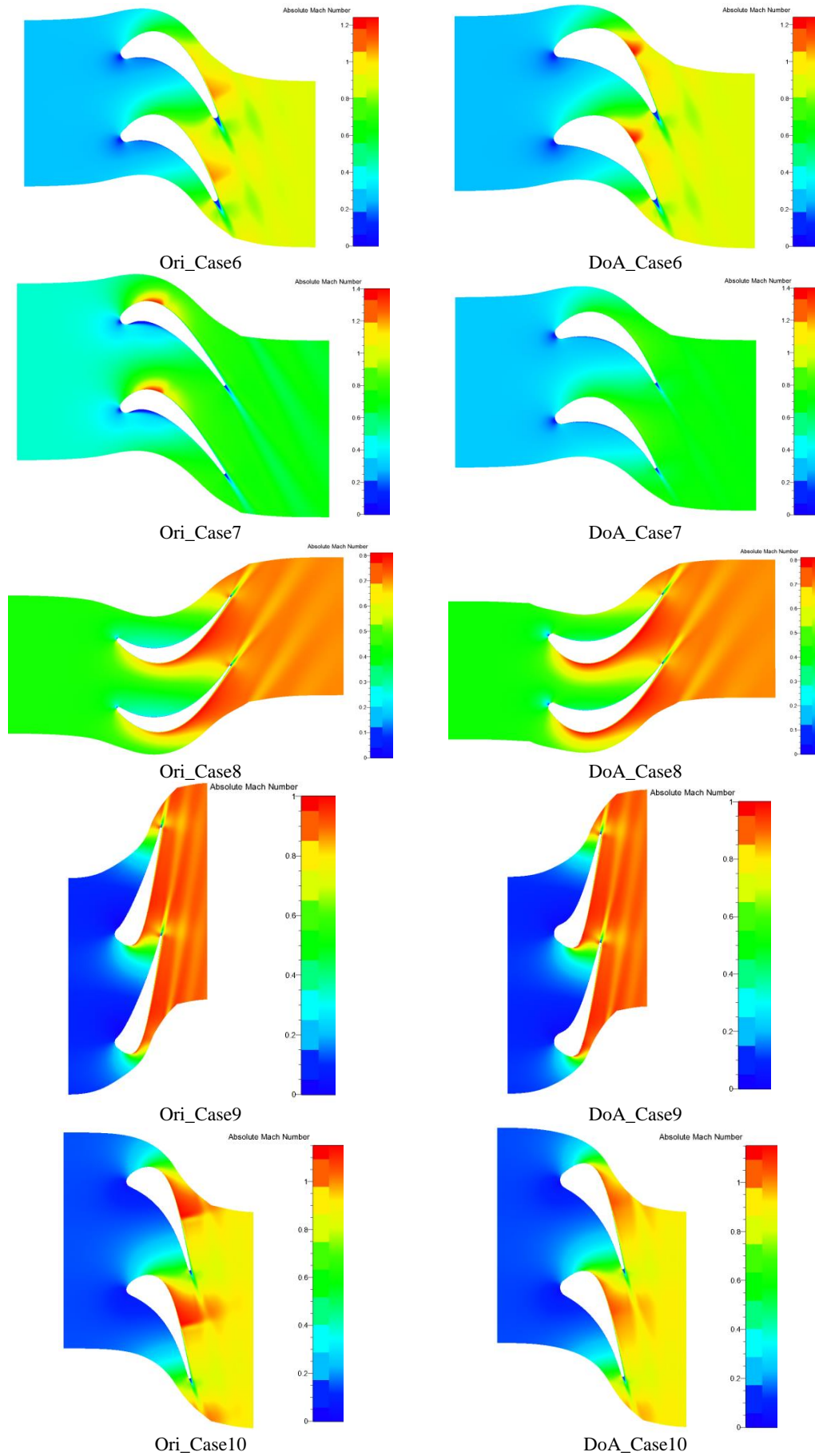
DoA_Case6

Ori_Case7

DoA_Case7

Ori_Case8

DoA_Case8

Ori_Case9

DoA_Case9

Ori_Case10

DoA_Case10

Fig. B Distributions of predicted Mach number at the midspan at design conditions.

REFERENCES

Anguita, D., C. Cravero, C. Filz and F. Rivieccio (2003). An Innovative Technique for the Aerodynamic Design of Turbine Profiles Using Artificial Intelligence. *In 33rd AIAA Fluid Dynamics Conference and Exhibit*. Orlando, Florida.

Aungier, R. H. (2006a). *Turbine Aerodynamics: Axial-Flow and Radial-Flow Turbine Design and Analysis.* New York, Chap. 6, 133-166.

Aungier, R. H. (2006b). *Turbine Aerodynamics: Axial-Flow and Radial-Flow Turbine Design and Analysis.* New York, Chap. 4, 61-92.

Behr, T. (2007). *Control of Rotor Tip Leakage and Secondary Flow by Casing Air Injection in Unshrouded Axial Turbines*. Ph.D. Thesis, ETH, Zurich.

Bryce, J. D., M. R. Litchfield and N. P. Leversuch (1985). The Design, Performance and Analysis of a High Work Capacity Transonic Turbine. *Journal of Engineering for Gas Turbines and Power* 107(4), 931-937.

Chatel, A., T. Verstraete and G. Coussement (2019). Multipoint Optimization of an Axial Turbine Cascade Using a Hybrid Algorithm. *ASME Paper*. No. GT2019-91471.

Clark, C. J. (2019). A Step Towards an Intelligent Aerodynamic Design Process. *ASME Paper*. No. GT2019-91637.

Colclough, C. D. (1966a). Design of Turbine Blades Suitable for Supersonic Relative Inlet Velocities and the Investigation of Their Performance in Cascades: Part I—Theory and Design. *ARCHIVE Journal of Mechanical Engineering Science 1959-1982 (1-23)* 8(1), 110–128.

Colclough, C. D. (1966b). Design of Turbine Blades Suitable for Supersonic Relative Inlet Velocities and the Investigation of Their Performance in Cascades: Part II—Experiments, Results and Discussion. *ARCHIVE Journal of Mechanical Engineering Science 1959-1982 (1-23)* 8(2), 185–197.

Deb, K., A. Pratap, S. Agarwal and T. Meyarivan (2002). A Fast and Elitist Multiobjective Genetic Algorithm: NSGA-II. *IEEE transactions on evolutionary computation* 6(2), 182–197.

Deb, K. and H. Jain (2013). An Evolutionary Many-objective Optimization Algorithm Using Reference-point-based Nondominated Sorting Approach, Part I: Solving Problems with Box Constraints. *IEEE transactions on evolutionary computation* 18(4), 577-601.

Drela, M. and M. B. Giles (1987). Viscous-inviscid Analysis of Transonic and Low Reynolds Number Airfoils. *AIAA Journal* 25(10), 1347–1355.

Giel, P. W. (2008). NASA/GE Highly-loaded Turbine Research Program. *AIAA Turbine Engine Testing Working Group Meeting*, Cleveland, Ohio.

Hodson, H. P. and R. G. Dominy (1987). The Off-Design Performance of a Low-Pressure Turbine Cascade. *Journal of Turbomachinery* 109(2), 201-209.

Jain, H. and K. Deb (2013). An Evolutionary Many-objective Optimization Algorithm Using Reference-point Based Nondominated Sorting Approach, Part II: Handling Constraints and Extending to an Adaptive Approach. *IEEE Transactions on Evolutionary Computation* 18(4), 602-622.

Kacker, S. C. and U. Okapuu (1982). A Mean Line Prediction Method for Axial Flow Turbine Efficiency. *Journal of Engineering for Power* 104(1), 111–119.

Kiock, R., F. Lehthaus, N. C. Baines and C. H. Sieverding (1986). The Transonic Flow Through a Plane Turbine Cascade as Measured in Four European Wind Tunnels. *Journal of Engineering for Gas Turbines and Power* 108(2), 277–284.

Klambauer, G., T. Unterthiner, A. Mayr and S. Hochreiter (2017). Self-Normalizing Neural Networks. *In Advances in Neural Information Processing Systems (NIPS)*. arXiv: 1706.02515

Kosowski, K., K. Tucki and A. Kosowski (2009). Turbine stage design aided by artificial intelligence methods. *Expert Systems with Applications* 36(9), 11536-11542.

Kosowski, K., K. Tucki and A. Kosowski (2010). Application of Artificial Neural Networks in Investigations of Steam Turbine Cascades. *Journal of Turbomachinery* 132(1), 014501.

Lee, S., S. Lee., K. Kim., D. Lee., Y. Kang and D. Rhee (2014). Optimization Framework Using Surrogate Model for Aerodynamically Improved 3D Turbine Blade Design. *ASME Paper*. No. GT2014-26571.

Li, Z. H. and X. Q. Zheng (2017). Review of Design Optimization Methods for Turbomachinery Aerodynamics. *Progress in Aerospace Sciences* 93, 1-23.

Meng, F. S., J. Gao, Q. Zheng, W. L. Fu and X. Z. Liu (2019). Experimental Study on Large Meridional Expansion Annular Sector Cascades with Variable Working Conditions. *Journal of Propulsion Technology* 40(5), 986-995.

Moroz, L., Y. Govoruschenko, L. Romanenko and P. Pagur (2004). Methods and Tools for Multidisciplinary Optimization of Axial Turbine Stages with Relatively Long Blades. *ASME Paper*. No. GT2004-53379.

Pierret, S. and R. A. Van den Braembussche (1999). Turbomachinery Blade Design Using a Navier–Stokes Solver and Artificial Neural Network. *Journal of Turbomachinery* 121(2), 326–332.

Pritchard, L. J. (1985). An Eleven Parameter Axial Turbine Airfoil Geometry Model. *ASME Paper*. No. 85-GT-219.

Shelton, M. L., B. A. Gregory, S. H. Lamson, H. L. Moses, R. L. Doughty and T. Kiss (1993). Optimization of a Transonic Turbine Airfoil Using Artificial Intelligence CFD and Cascade Testing. *ASME Paper*. No. 93-GT-161.

Sonoda, T., T. Arima, M. Olhofer, B. Sendhoff, F. Kost and P. A. Giess (2006). A Study of Advanced High-loaded Transonic Turbine Airfoils. *Journal of Turbomachinery*. 128(4), 650-657.

Thulin, R. D., D. C. Howe and I. D. Singer (1982). Energy Efficient Engine High-pressure Turbine Detailed Design Report. *NASA Report*. NASA-CR-165608.

Tsujita, H. and M. Kaneko (2019). Profile Loss of Ultra-Highly Loaded Turbine Cascade at Transonic Flow Condition. *ASME Paper*. No. GT-2019-91264.

Waesker. M., B. Buelten., N. Kienzle and C. Doetsch (2020). Optimization of Supersonic Axial Turbine Blades Based on Surrogate Models. *ASME Paper*. No. GT2020-14465

Youngren, H. H. (1991). *Analysis and Design of Transonic Cascades with Splitter Vanes*. Ph.D. thesis, Massachusettes Institute of Technology, Cambridge, US.